

between 0.2 and 1.0 in nestlings. As not all individuals were typed with the same set of microsatellite markers, we calculated standardized individual heterozygosity¹⁰ (proportion of heterozygous loci/mean heterozygosity of typed loci). This measure is used in all analyses and is referred to as 'individual heterozygosity' for simplicity. We also calculated two other, previously suggested measures of individual genetic diversity: internal relatedness¹⁰ and mean d^2 -value²⁹ where d^2 is the squared length difference between the alleles at a locus. Heterozygosity, standardized heterozygosity and internal relatedness were highly correlated (all $r > 0.89$, $P < 0.0001$) and all three measures led to similar conclusions (data not shown). Mean d^2 -values were weakly correlated with the other measures ($r = 0.24$ – 0.32 , all $P < 0.0001$) and explained comparatively little variation in individual fitness.

The assumption that heterozygosity measured at a limited number of loci reflects genome-wide heterozygosity can be questioned³⁰. Any relationship between average heterozygosity and fitness might be due to close linkage between a microsatellite locus and loci coding for fitness-related traits. To check whether the effect of overall heterozygosity on fitness depended on one or a few of the microsatellite loci, we repeated all analyses for each locus separately (data not shown). Heterozygosity at six out of seven loci significantly affected at least one fitness measure, and different fitness measures were predicted by heterozygosity at different loci, so we only present data on overall heterozygosity.

We calculated pairwise relatedness between partners using Relatedness 5.0 (<http://www.gsoftnet.us/GSoft.html>). The average relatedness between adult males and females (expected $r = 0$) in our study population was -0.0007 (s.e.m. calculated by 'jack-knifing' over loci = 0.0009). In a random sample of 100 broods, the average relatedness among full siblings (expected $r = 0.5$) was 0.47 (s.e.m. = 0.02). The mean inbreeding coefficient of our population (F_{is}), calculated from the microsatellite data using Fstat V2.9.3, equals -0.006 . The observed level of inbreeding was 3.3%: two of 61 local recruits (with known parents) mated with close relatives ($r = 0.5$ and 0.125).

Received 21 March; accepted 25 July 2003; doi:10.1038/nature01969.

1. Jennions, M. D. & Petrie, M. Why do females mate multiply? A review of the genetic benefits. *Biol. Rev.* **75**, 21–64 (2000).
2. Tregenza, T. & Wedell, N. Genetic compatibility, mate choice and patterns of parentage: invited review. *Mol. Ecol.* **9**, 1013–1027 (2000).
3. Zeh, J. A. & Zeh, D. W. Reproductive mode and the genetic benefits of polyandry. *Anim. Behav.* **61**, 1051–1063 (2001).
4. Brown, J. L. A theory of mate choice based on heterozygosity. *Behav. Ecol.* **8**, 60–65 (1997).
5. Zeh, J. A. & Zeh, D. W. The evolution of polyandry I: intragenomic conflict and genetic incompatibility. *Proc. R. Soc. Lond. B* **263**, 1711–1717 (1996).
6. Tregenza, T. & Wedell, N. Polyandrous females avoid costs of inbreeding. *Nature* **415**, 71–73 (2002).
7. Thornhill, N. W. *The Natural History of Inbreeding and Outbreeding: Theoretical and Empirical Perspectives* (Univ. Chicago Press, Chicago, 1993).
8. Kempnaers, B., Adriaens, E., van Noordwijk, A. J. & Dhondt, A. A. Genetic similarity, inbreeding and hatching failure in blue tits: are unhatched eggs infertile? *Proc. R. Soc. Lond. B* **263**, 179–185 (1996).
9. Coltman, D. W., Bowen, W. D. & Wright, J. M. Birth weight and neonatal survival of harbour seal pups are positively correlated with genetic variation measured by microsatellites. *Proc. R. Soc. Lond. B* **265**, 803–809 (1998).
10. Amos, W. *et al.* The influence of parental relatedness on reproductive success. *Proc. R. Soc. Lond. B* **268**, 2021–2027 (2001).
11. Hansson, B., Bensch, S., Hasselquist, D. & Akesson, M. Microsatellite diversity predicts recruitment of sibling great reed warblers. *Proc. R. Soc. Lond. B* **268**, 1287–1291 (2001).
12. Höglund, J. *et al.* Inbreeding depression and male fitness in black grouse. *Proc. R. Soc. Lond. B* **269**, 711–715 (2002).
13. Hansson, B. & Westerberg, L. On the correlation between heterozygosity and fitness in natural populations. *Mol. Ecol.* **11**, 2467–2474 (2002).
14. Pusey, A. & Wolf, M. Inbreeding avoidance in animals. *Trends Ecol. Evol.* **11**, 201–206 (1996).
15. Petrie, M. & Kempnaers, B. Extra-pair paternity in birds: explaining variation between species and populations. *Trends Ecol. Evol.* **13**, 52–58 (1998).
16. Blomqvist, D. *et al.* Genetic similarity between mates and extra-pair parentage in three species of shorebirds. *Nature* **419**, 613–615 (2002).
17. Kempnaers, B. *et al.* Extra-pair paternity results from female preference for high-quality males in the blue tit. *Nature* **357**, 494–496 (1992).
18. Kempnaers, B., Verheyen, G. R. & Dhondt, A. A. Extrapair paternity in the blue tit (*Parus caeruleus*): female choice, male characteristics, and offspring performance. *Behav. Ecol.* **8**, 481–492 (1997).
19. Aparicio, J. M., Cordero, P. J. & Veiga, J. P. A test of the hypothesis of mate choice based on heterozygosity in the spotless starling. *Anim. Behav.* **62**, 1001–1006 (2001).
20. Andersson, S., Örnborg, J. & Andersson, M. Ultraviolet sexual dimorphism and assortative mating in blue tits. *Proc. R. Soc. Lond. B* **265**, 445–450 (1998).
21. Hunt, S., Cuthill, I. C., Bennett, A. T. D. & Griffiths, R. Preferences for ultraviolet partners in the blue tit. *Anim. Behav.* **58**, 809–815 (1999).
22. Sheldon, B., Andersson, S., Griffith, S. C., Örnborg, J. & Sendecka, J. Ultraviolet colour variation influences blue tit sex ratios. *Nature* **402**, 874–877 (1999).
23. Mitton, J. B., Schuster, W. S. F., Cothran, E. G. & De Fries, J. C. Correlation between the individual heterozygosity of parents and their offspring. *Heredity* **71**, 59–63 (1993).
24. Stockley, P., Searle, J. B., MacDonald, D. W. & Jones, C. S. Female multiple mating behaviour in the common shrew as a strategy to reduce inbreeding. *Proc. R. Soc. Lond. B* **254**, 173–179 (1993).
25. Dawson, D. A., Hanotte, O., Greig, C., Stewart, I. R. K. & Burke, T. Polymorphic microsatellites in the blue tit *Parus caeruleus* and their cross-species utility in 20 songbird families. *Mol. Ecol.* **9**, 1941–1944 (2000).
26. Bensch, S., Price, T. & Kohn, J. Isolation and characterization of microsatellite loci in a *Phylloscopus* warbler. *Mol. Ecol.* **6**, 91–92 (1997).
27. Fridolfsson, A. K., Gyllenstein, U. B. & Jakobsson, S. Microsatellite markers for paternity testing in the willow warbler *Phylloscopus trochilus*: high frequency of extra-pair young in an island population. *Heredity* **126**, 127–132 (1997).
28. Jamieson, A. The effectiveness of using co-dominant polymorphic allelic series for (1) checking

- pedigrees and (2) distinguishing full-sib pair members. *Anim. Genet.* **25**, 37–44 (1994).
29. Pemberton, J. M., Coltman, D. W., Coulson, T. N. & Slate, J. in *Microsatellites, Evolution and Applications* (eds Goldstein, D. B. & Schlotterer, C.) 151–164 (Oxford Univ. Press, Oxford, 1999).
30. Turelli, M. & Ginzburg, L. R. Should individual fitness increase with heterozygosity? *Genetics* **104**, 191–209 (1983).

Acknowledgements We thank D. Blomqvist, S. Griffith, D. Hasselquist, L. Keller, M. Milinski, A. Peters, B. Sheldon, C. Wedekind and D. Zeh for comments on the manuscript; K. Carter, D. Kaulfuss, H. Kunc, K. Peer, A. Pösel and A. Türk for help with field and laboratory work; S. Andersson for computing the colour variables; and H. Winkler (Konrad Lorenz Institute for Comparative Ethology) and R.-T. Klumpp and A. Fojt (Institute of Silviculture, University of Agricultural Sciences, Vienna) for logistic support.

Competing interests statement The authors declare that they have no competing financial interests.

Correspondence and requests for materials should be addressed to B.K. (b.kempnaers@erl.ornithol.mpg.de).

RNA molecules stimulate prion protein conversion

Nathan R. Deleault, Ralf W. Lucassen & Surachai Supattapone

Department of Biochemistry, 7200 Vail Building, Dartmouth Medical School, Hanover, New Hampshire 03755, USA

Much evidence supports the hypothesis that the infectious agents of prion diseases are devoid of nucleic acid, and instead are composed of a specific infectious protein¹. This protein, PrP^{Sc}, seems to be generated by template-induced conformational change of a normally expressed glycoprotein, PrP^C (ref. 2). Although numerous studies have established the conversion of PrP^C to PrP^{Sc} as the central pathogenic event of prion disease, it is unknown whether cellular factors other than PrP^C might be required to stimulate efficient PrP^{Sc} production. We investigated the biochemical amplification of protease-resistant PrP^{Sc}-like protein (PrPres) using a modified version³ of the protein-misfolding cyclic amplification method⁴. Here we report that stoichiometric transformation of PrP^C to PrPres *in vitro* requires specific RNA molecules. Notably, whereas mammalian RNA preparations stimulate *in vitro* amplification of PrPres, RNA preparations from invertebrate species do not. Our findings suggest that host-encoded stimulatory RNA molecules may have a role in the pathogenesis of prion disease. They also provide a practical approach to improve the sensitivity of diagnostic techniques based on PrPres amplification.

We previously showed that PrPres amplification *in vitro* shares many specific features with the pathogenic process of prion propagation *in vivo*, including strain and species specificity³. In a typical amplification reaction, diluted prion-infected brain homogenate (0.1% w/v) is mixed with either 5% (w/v) normal brain homogenate or buffer control and incubated overnight at 37 °C. Hamster Sc237 PrPres is amplified about sixfold under these conditions (Fig. 1a, compare M with Sc). While characterizing the biochemical requirements of PrPres amplification reactions, we were surprised to discover that treatment of such reactions with DNase-free, heterogeneous pancreatic RNase abolished PrPres amplification in a dose-dependent manner (Fig. 1a, first panel). *In vitro* PrPres amplification was also abolished by treatment with purified pancreatic RNase A, RNase T1, micrococcal nuclease, or benzonase (Fig. 1a). In a control experiment, we found that addition of RNase A for 1 h after overnight incubation did not reduce the recovery of PrPres already amplified (Supplementary Fig. S1).

By contrast, PrPres amplification was not affected by addition of

RNase V1, which degrades only double-stranded (ds)RNA molecules⁵, or RNase H, which specifically cleaves RNA:DNA hybrids⁶ (Fig. 1b, first and second panels). Taken together, these results suggest that single-stranded (ss)RNA is required for PrPres amplification *in vitro*, but that dsRNA and RNA:DNA hybrids are not. Addition of DNase or the restriction enzyme *EcoRI* did not decrease PrPres amplification, showing that DNA is not required for the process (Fig. 1b, third and fourth panels). Addition of the enzymes apyrase and heparinase III also had no effect on PrPres amplification, suggesting that neither high-energy nucleotides nor molecules containing heparan sulphate are required for PrPres amplification *in vitro* (Fig. 1b, fifth and sixth panels). In control experiments, we confirmed the degradation of the target molecules in each of these reaction mixtures by using appropriate analytical assays for these structures (Supplementary Fig. S2).

To ensure that the commercial nuclease preparations we used were not contaminated with proteases, we measured the levels of PrP^C and PrPres after overnight incubation with various nucleases. These measurements confirmed that levels of PrP^C (Fig. 2a) and input PrPres (Fig. 2b) were both unperturbed by addition of enzymes that inhibited PrPres amplification.

As a control to confirm that abolition of PrPres amplification depends on the stimulatory activity of each inhibitory nuclease, we

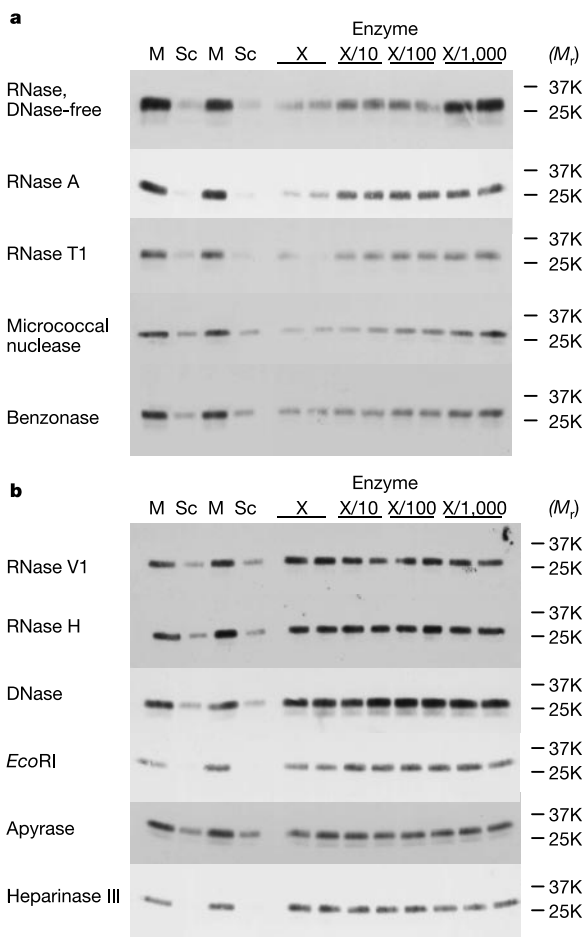


Figure 1 Effect of various enzymes on PrPres amplification. Immunoblots of PrPres amplification reactions. Samples include mixtures of normal and diluted scrapie brain homogenate (M), diluted scrapie brain homogenate control (Sc), and mixtures of normal and diluted scrapie brain homogenate incubated with various enzymes in a dilution series. The values of X (manufacturer's $U \mu l^{-1}$) for enzymes are: DNase-free RNase = 0.5; RNase A = 0.005; RNase T1 = 50; micrococcal nuclease = 0.005; benzonase = 2.5; RNase V1 = 0.01; RNase H = 1; RNase-free DNase = 1; *EcoRI* = 1; apyrase = 0.1; heparinase III = 0.025.

added benzonase, micrococcal nuclease and RNase A to PrPres amplification reactions in enzymatically inactive states. Both benzonase and micrococcal nuclease require divalent cations for enzymatic activity, so we inactivated these nucleases by addition of 5 mM EDTA. The active site of RNase A contains a critical histidine residue that can be covalently modified by diethyl pyrocarbonate (DEPC). Therefore, we pre-treated RNase A with DEPC to inhibit its RNase activity, and removed excess DEPC by dialysis. Our results show that none of the three nucleases inhibits PrPres amplification in their inactive states, supporting the hypothesis that intact RNA molecules stimulate this process (Fig. 2c).

To test whether inhibition of PrPres amplification might be mediated by end products of RNase digestion, we measured directly the effect of cyclic 2',3'-guanine monophosphate (GMP) and 3'-cytidine monophosphate (CMP) on PrPres amplification. Neither of these nucleotides inhibited PrPres amplification *in vitro* at concentrations up to 1 mM (Fig. 2d). Our control experiments rule out the possibility that contaminating proteases, steric hindrance, or digestion end-products account for the inhibition of

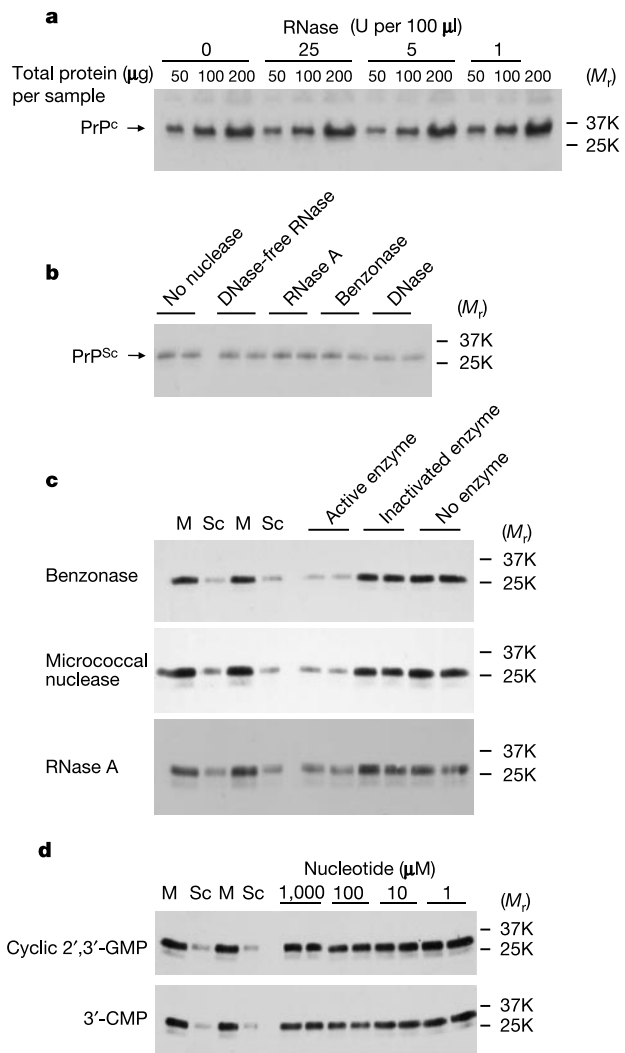


Figure 2 Nucleases do not cause proteolytic, steric or end-product inhibition of PrPres amplification. **a**, Effect of DNase-free RNase on PrP^C levels. Standard amplification mixtures were incubated overnight with RNase. Serial dilutions of each sample are shown. **b**, Effect of nucleases on PrPres levels. Samples of diluted scrapie brain homogenate were treated with specified nucleases at concentrations designated 'X' in Fig. 1. **c**, Effect of inactivated nucleases on PrPres amplification. Samples include mixtures of normal and diluted scrapie brain homogenate (M) and diluted scrapie brain homogenate control (Sc). **d**, Effect of nucleotides on PrPres amplification.

PrPres amplification by specific nucleases. Taken together, these experiments indicate that RNA is required for PrPres amplification *in vitro*.

We next sought to determine whether a preparation of isolated RNA molecules could reconstitute the ability of nuclease-treated normal brain homogenate to amplify PrPres. Remarkably, total RNA isolated from hamster brain successfully reconstituted the ability of benzonase-pre-treated brain homogenate to amplify PrPres in a dose-dependent manner (Fig. 3a). By contrast, purified heparan sulphate proteoglycan (HSPG) failed to reconstitute PrPres amplification (Fig. 3a). Other polyanions, such as ssDNA (Fig. 3b), polyadenylic acid, heparan sulphate, pentosan sulphate and polyglutamic acid (data not shown) also failed to stimulate PrPres amplification. In this and other reconstitution experiments, benzonase-treated control lanes have a greater level of PrPres amplification than the diluted scrapie brain homogenate control samples, indicating that the benzonase pre-treatment reactions were incomplete. Empirically, we found that it was necessary to perform benzonase pre-treatment reactions at 4°C to avoid denaturing PrP^C before the addition of polyanions.

To estimate the molecular size of the RNA species capable of reconstituting PrPres amplification, we fractionated our preparation of total hamster brain RNA by ultrafiltration through a filter with a relative molecular mass cutoff of approximately 100,000 (M_r , 100K). Using agarose gel electrophoresis, we detected all of the ribosomal RNA bands in the retentate and all of the transfer RNA in the filtrate (data not shown). Using these samples, we discovered that the filter retentate was capable of reconstituting PrPres amplification to a level slightly lower than unfractionated total brain RNA. By contrast, the filtrate was not able to reconstitute PrPres amplification (Fig. 3c). These data indicate that most of the reconstitution activity is conferred by RNA molecules >100K in size (>300 nucleotides).

There is currently a need to develop more sensitive diagnostic tests for prion disease—this might be achieved by increasing the efficiency of PrPres amplification techniques. We therefore investigated whether addition of total hamster brain RNA could increase the efficiency of PrPres amplification *in vitro* in brain samples not

pre-treated with nuclease. We mixed a more dilute homogenate of prion-infected brain (0.02% w/v) with 5% (w/v) normal brain homogenate overnight without sonication, and measured PrPres amplification. Our results show that addition of total hamster brain RNA to this mixture of intact brain homogenates significantly stimulates PrPres amplification over baseline (Fig. 4a). As a control, we confirmed that addition of RNA did not alter the level of input PrPres or PrP^C in these samples (Supplementary Fig. S3). Densitometric measurements indicate that PrPres in 0.02% (w/v) prion-infected brain homogenate samples is amplified about sixfold after overnight incubation, similar to the PrPres amplification level previously reported for 0.1% (w/v) prion-infected brain homogenate³. By contrast, PrPres in samples amplified with RNA is amplified about 24-fold, indicating that addition of RNA increases the efficiency of *in vitro* PrPres amplification about fourfold. Addition of RNA also increased the efficiency of PrPres amplification of sonicated protein-misfolding cyclic amplification (PMCA) reactions (Supplementary Fig. S4).

To assess the specificity of RNA-mediated stimulation of PrPres amplification, we isolated total RNA from several sources, including *Escherichia coli*, *Saccharomyces cerevisiae*, *Caenorhabditis elegans*, *Drosophila melanogaster*, and mouse and hamster brain. Agarose gel electrophoresis analysis of these preparations revealed the expected band patterns for each species and confirmed that each preparation

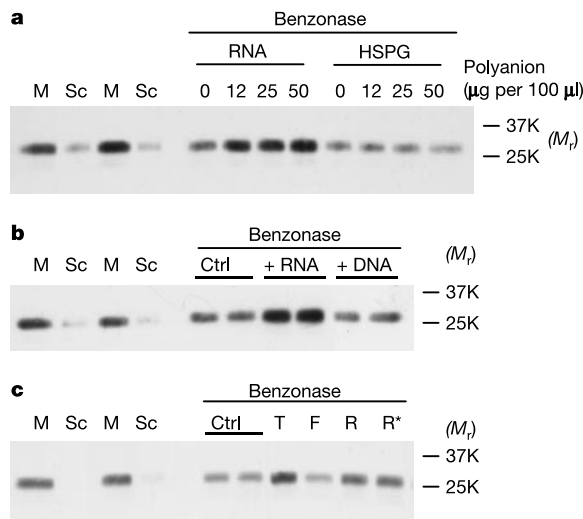


Figure 3 Reconstitution of PrPres amplification with RNA. Immunoblots of PrPres amplification reactions. Samples include mixtures of normal and diluted scrapie brain homogenate (M) and diluted scrapie brain homogenate control (Sc). Indicated samples were pre-treated with benzonase before reconstitution assays as described in Methods. **a**, Reconstitution with total hamster brain RNA or HSPG. **b**, Reconstitution with 0.5 mg ml⁻¹ total hamster brain RNA or 0.5 mg ml⁻¹ random, synthetic 23-base DNA oligonucleotide. **c**, Reconstitution with 0.5 mg ml⁻¹ total (T), filtrate (F), retentate (R) and 50% formamide retentate (R*) samples from RNA fractionated by ultrafiltration.

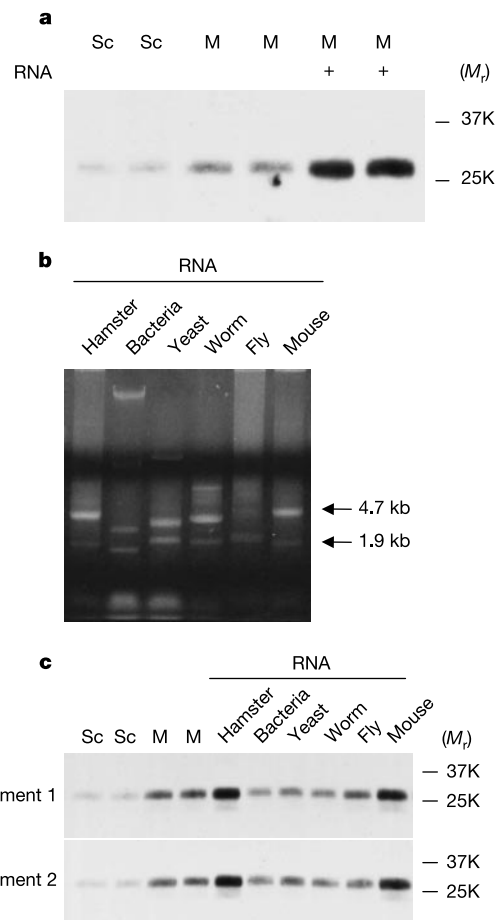


Figure 4 Stimulation of PrPres amplification with RNA. **a**, Immunoblot of PrPres amplification reactions. Samples include mixtures of 5% (w/v) normal and 0.02% (w/v) scrapie brain homogenate (M) and diluted scrapie brain homogenate control (Sc). Indicated samples contained 0.5 mg ml⁻¹ total hamster brain RNA (+). **b**, Agarose gel electrophoresis of total RNA prepared from various species. **c**, Immunoblot of species-specific stimulation of PrPres amplification with RNA. Total RNA (0.5 mg ml⁻¹) prepared from various species was added to PrPres amplification reactions.

contained high-quality, non-degraded RNA (Fig. 4b). Furthermore, each of these preparations was substantially free from contaminants as judged by optical spectroscopy ($A_{260}/A_{280} > 1.9$; where A indicates absorbance and subscript numbers indicate wavelength). Notably, among the six preparations of RNA tested, only hamster and mouse brain RNA could stimulate PrPres amplification *in vitro* (Fig. 4c). This apparent species specificity cannot be attributed to tissue specificity because total hamster liver RNA also stimulated PrPres amplification (data not shown). This argues that mice and hamsters express specific RNA molecules required for PrPres amplification. Additional experiments show that the RNA stimulation activity within the Trizol-extracted hamster brain RNA preparation was irreversibly destroyed by glyoxylation, but not by deproteination, heating to 60 °C, or transient exposure to 50% formamide for 1 h (Supplementary Fig. S5).

If PrPres amplification studies accurately model PrP^{Sc} formation *in vivo*, the results presented here represent a significant advance in our understanding of the mechanism of prion conversion. Previously, it has been shown that purified PrP^C can be converted into protease-resistant PrPres *in vitro* in the absence of cellular cofactors⁷. However, the fact that a 50-fold molar excess of purified PrPres is required to drive conversion of purified PrP^C suggests that efficient PrPres formation may depend on the presence of cellular factors other than PrP^C (ref. 8). On the basis of the results presented here, we propose the hypothesis that specific RNA molecules are cellular cofactors for PrP^{Sc} formation. Consistent with our hypothesis that specific RNA-converting factors stimulate PrP^{Sc} formation, nucleic acids bind avidly to and promote conformational change of recombinant PrP (refs 9–14). However, it is important to note that full-length, refolded recombinant PrP lacking post-translational modifications cannot undergo stoichiometric conversion to PrPres (Supplementary Fig. S6), and therefore the results of biophysical studies using recombinant PrP cannot be directly related to the results described here. It has been proposed that PrP^{Sc} molecules might bind to specific host RNA molecules to generate strain diversity¹⁵. Whether the RNA-converting factors we describe are also involved in generating strain diversity remains to be determined. Finally, it is important to emphasize that the existence of RNA-converting factors is fully consistent with the protein-only hypothesis proposed previously¹, because the nucleic acids we describe are host-encoded and not contained within the infectious agent. □

Methods

Animal and reagent sources

Specific-pathogen-free female golden Syrian hamsters at 3 weeks old were purchased from Charles River Laboratories. Apyrase, DEPC, cyclic 2',3'-GMP, 3'-CMP, heparinase III, heparan sulphate proteoglycan ($M_r > 200K$), polyadenylic acid (M_r 200–2,000K) and polyglutamic acid (M_r 50–100K) were obtained from Sigma; RNase-free DNase, micrococcal nuclease, RNase A and DNase-free RNase were obtained from Roche; RNase T1 was obtained from Epicentre; recombinant benzonase nuclease was purchased from Novagen; EcoRI was obtained from Gibco BRL; and RNase H and RNase V1 were obtained from Ambion.

In vitro PrPres amplification

In vitro PrPres amplification³ and PMCA⁴ were performed as previously described, except that normal brain homogenates were prepared with EDTA-free complete protease inhibitors (Roche) to facilitate experiments involving metal-dependent enzymes. Two millimolar MgCl₂ was added to reactions with benzonase and 2 mM CaCl₂ was added to reactions with micrococcal nuclease and apyrase. All amplification and control reactions were performed at 37 °C for 16 h. For PrPres detection, protease digestion was performed with 50 µg ml⁻¹ proteinase K for 1 h at 37 °C and immunoblotting was performed with 3F4 monoclonal antibody (Signet). For PrP^C detection, samples were not subjected to proteinase K digestion before immunoblotting. All protein electrophoresis experiments shown were performed on 12% SDS polyacrylamide gels and reference M_r for such experiments are shown.

Nuclease inactivation

Micrococcal nuclease and benzonase were inhibited with 5 mM EDTA. RNase A (50 µg) was incubated with 1% DEPC in 100 µl at 25 °C for 2 h. After incubation, the reaction was dialysed twice against 1 l 10 mM Tris pH 7.2 at 4 °C using a Pierce 3500 MW Slide-A-Lyzer

minidialysis unit to remove free DEPC. Control samples containing active RNase A were dialysed in parallel. Protein recovery >90% was confirmed by BCA assay (Pierce). Active and inactivated nucleases were added to amplification reactions at concentrations designated 'X' in Fig. 1. 'No enzyme' control samples were processed in parallel.

Reconstitution assays

Nuclease digestion before reconstitution was performed by incubating a batch of normal brain homogenate (10% w/v) with benzonase (final concentration of 2.5 U µl⁻¹) and 2 mM MgCl₂ for 16 h at 4 °C in the absence of detergents. Benzonase was then inactivated by the addition of 5 mM EDTA before reconstitution with RNA or other polyanions.

Preparation and measurement of RNA

RNA was isolated from animals <5 min after death using rotor–stator homogenization, extraction with Trizol reagent (Invitrogen) for 5 min at 25 °C, and isopropanol precipitation according to manufacturer's instructions, using RNase-free reagents, containers and equipment. For yeast, cell walls were disrupted during extraction as previously described, using Trizol in place of phenol¹⁶. All RNA solutions were alcohol precipitated, washed and resuspended in RNase-free water before use. The concentration and purity of each solution was determined by spectroscopic measurement of absorbance at $\lambda_1/\lambda_2 = 260/280$ nm and confirmed by electrophoresis on 1% agarose gels stained with ethidium bromide.

RNA size fractionation

Total hamster brain RNA (0.4 mg) was diluted into 0.8 ml RNase-free water, loaded in 0.2-ml batches onto four separate Schleicher and Schuell Centrex UF-05 (100K cutoff) ultrafiltration devices, and centrifuged for 15 min at 3,000g. The devices were then washed with an equal volume of water. The filtrates were pooled and retentate fractions collected by briefly centrifuging the ultrafiltration devices upside down into new microcentrifuge tubes. Parallel samples of denatured retentate were prepared in 50% formamide to disrupt all intra- and intermolecular interactions.

Reverse transcriptase polymerase chain reaction

RT-PCR was performed using the One Step RNA PCR kit (AMV) from Takara/Fisher following the manufacturer's instructions, using the PrP-specific primers 5'-CGAACC TTGGCTACTGGCTGCTG-3' and 5'-GCTTGATGGTGATATTGACGCGATC-3', and the following parameters: reverse transcription at 50 °C for 15 min, heat inactivation of reverse transcriptase at 94 °C for 2 min, ×25 PCR cycles (94 °C for 30 s, 55 °C for 30 s, 72 °C for 90 s). Products were run on a 1% agarose gel and stained with ethidium bromide.

Received 4 July; accepted 31 July 2003; doi:10.1038/nature01979.

1. Prusiner, S. B. Novel proteinaceous infectious particles cause scrapie. *Science* **216**, 136–144 (1982).
2. Prusiner, S. B. (ed.) *Prion Biology and Diseases* (Cold Spring Harbor Laboratory Press, Cold Spring Harbor, New York, 1999).
3. Lucassen, R., Nishina, K. & Supattapone, S. *In vitro* amplification of protease-resistant prion protein requires free sulfhydryl groups. *Biochemistry* **42**, 4127–4135 (2003).
4. Saborio, G. P., Permanne, B. & Soto, C. Sensitive detection of pathological prion protein by cyclic amplification of protein misfolding. *Nature* **411**, 810–813 (2001).
5. Lockard, R. E. & Kumar, A. Mapping tRNA structure in solution using double-strand-specific ribonuclease V1 from cobra venom. *Nucleic Acids Res.* **9**, 5125–5140 (1981).
6. Banks, G. R. A ribonuclease H from *Ustilago maydis*. Properties, mode of action and substrate specificity of the enzyme. *Eur. J. Biochem.* **47**, 499–507 (1974).
7. Kocisko, D. A. *et al.* Cell-free formation of protease-resistant prion protein. *Nature* **370**, 471–474 (1994).
8. Caughey, B., Horiuchi, M., Demaimay, R. & Raymond, G. J. Assays of protease-resistant prion protein and its formation. *Methods Enzymol.* **309**, 122–133 (1999).
9. Derrington, E. *et al.* PrPC has nucleic acid chaperoning properties similar to the nucleocapsid protein of HIV-1. *C. R. Acad. Sci. III* **325**, 17–23 (2002).
10. Moscardini, M. *et al.* Functional interactions of nucleocapsid protein of feline immunodeficiency virus and cellular prion protein with the viral RNA. *J. Mol. Biol.* **318**, 149–159 (2002).
11. Gabus, C. *et al.* The prion protein has RNA binding and chaperoning properties characteristic of nucleocapsid protein NCP7 of HIV-1. *J. Biol. Chem.* **276**, 19301–19309 (2001).
12. Gabus, C. *et al.* The prion protein has DNA strand transfer properties similar to retroviral nucleocapsid protein. *J. Mol. Biol.* **307**, 1011–1021 (2001).
13. Nandi, P. K., Leclerc, E., Nicole, J. C. & Takahashi, M. DNA-induced partial unfolding of prion protein leads to its polymerisation to amyloid. *J. Mol. Biol.* **322**, 153–161 (2002).
14. Cordeiro, Y. *et al.* DNA converts cellular prion protein into the β -sheet conformation and inhibits prion peptide aggregation. *J. Biol. Chem.* **276**, 49400–49409 (2001).
15. Weissmann, C. A 'unified theory' of prion propagation. *Nature* **352**, 679–683 (1991).
16. Chapon, C., Cech, T. R. & Zaugg, A. J. Polyadenylation of telomerase RNA in budding yeast. *RNA* **3**, 1337–1351 (1997).

Supplementary Information accompanies the paper on www.nature.com/nature.

Acknowledgements The authors thank G. Saborio, C. Soto, V. Ambros, C. Cole and W. Wickner for helpful advice. This work was supported by the Burroughs Wellcome Fund Career Development Award, the Hitchcock Foundation, and an NIH Clinical Investigator Development Award.

Competing interests statement The authors declare that they have no competing financial interests.

Correspondence and requests for materials should be addressed to S.S. (supattapone@dartmouth.edu).